

Three- and four-particle transfer strengths to states in ^{15}N

L. H. Harwood* and K. W. Kemper

Department of Physics, Florida State University, Tallahassee, Florida 32306

(Received 3 April 1979)

The 9.155, 9.83, and 10.69 MeV states in ^{15}N are found to have large cross sections in both three- and four-particle transfer reactions from a study of the $^{12}\text{C}(^7\text{Li}, \alpha\gamma)$, $^{12}\text{C}(^6\text{Li}, ^3\text{He}\gamma)$, and $^{11}\text{B}(^7\text{Li}, t\gamma)$ reactions at $E_{\text{Li}} = 28, 34,$ and 28 MeV, respectively. These results are in disagreement with simple cluster model arguments. Doppler shift attenuation measurements of the lifetimes of the ^{15}N states show that neither the weak-coupling shell model nor the cluster model accurately predicts the electromagnetic decay strengths in ^{15}N .

NUCLEAR STRUCTURE $^{12}\text{C}(^7\text{Li}, \alpha\gamma)$, $^{11}\text{B}(^7\text{Li}, t\gamma)$, $E = 28$ MeV, $^{12}\text{C}(^6\text{Li}, ^3\text{He}\gamma)$, $E = 34$ MeV; particle- γ coincidence; Ge(Li) detectors; measured relative cross sections for all states below 10.8 MeV excitation; measured lifetimes; measured γ -ray branching ratios; compared results to cluster and shell models.

I. INTRODUCTION

Clustering in nuclei has been of interest in nuclear physics for some time, and has recently been proposed as the underlying structure of the mirror states in ^{15}N and ^{15}O selectively populated in three-particle transfer reactions.¹ Buck, Dover, and Vary² have carried out calculations of the ^{15}N spectrum using a $t + ^{12}\text{C}$ cluster model. Their analysis was hampered by the lack of definitive spin-parity assignments for the states above 11 MeV excitation. The states below 11 MeV excitation are often members of close-lying doublets. The poor experimental energy resolution of the three-particle transfer reaction studies makes correlation of the strongly populated lower energy states with previously known states impossible. Also, some of the higher-lying states which appeared to be singlets in the early data are now known to be doublets. Thus, the interpretation of the transfer reaction's spectra has been difficult.

In the mass 19 system it has been possible to assign the states populated by four- and three-particle transfer reactions to α and triton cluster bands.³ A logical extension of the cluster concept would be ^{15}N states based on an $\alpha + ^{11}\text{B}$ configuration. As in the three-particle transfer reactions, the exact states populated in the four-particle transfer reactions are not known from the transfer work because of the high density of states in ^{15}N .

The present particle- γ coincidence study was undertaken to identify the states populated in the $^{12}\text{C}(^6\text{Li}, ^3\text{He})$, $^{12}\text{C}(^7\text{Li}, \alpha)$, and $^{11}\text{B}(^7\text{Li}, t)$ reactions by examining their γ decays. The first two reactions were chosen to compare two "triton" transfer reactions. If the same states are populated in both, then the idea that the final state nuclear structure is responsible for the observed selec-

tivity is supported. The last reaction was investigated to determine whether the same states are populated in the "triton" and " α -particle" transfer reactions. Lifetimes of the states were determined with the $^{12}\text{C}(^7\text{Li}, \alpha)$ reaction. The results of the measurements are compared with simple $^{12}\text{C} + t$ and $^{11}\text{B} + \alpha$ cluster models as well as the weak-coupling shell model.

II. EXPERIMENTAL PROCEDURE

The $^{12}\text{C}(^6\text{Li}, ^3\text{He}\gamma)^{15}\text{N}$ and $^{12}\text{C}(^7\text{Li}, \alpha\gamma)^{15}\text{N}$ measurements at $E_{\text{Li}} = 34$ and 28 MeV, respectively, reported in this work were carried out in a small volume chamber. The particles were detected by a $\Delta E \times E$ counter telescope consisting of 75 and 700 μm Si surface barrier detectors. The 700 μm detector was replaced by a 4 mm Si(Li) detector for the $^{11}\text{B}(^7\text{Li}, t\gamma)$ measurements at $E_{\text{Li}} = 28$ MeV. The telescope subtended a solid angle of 9.3 ± 0.5 msr and a polar half angle of $3.2^\circ \pm 0.2^\circ$; it was placed at 15° relative to the beam for the $^{12}\text{C}(^7\text{Li}, \alpha\gamma)$ and $^{11}\text{B}(^7\text{Li}, t\gamma)$ studies and at 20° for the $^{12}\text{C}(^6\text{Li}, ^3\text{He}\gamma)$ study. The detectors were cooled to -30°C .

The Li beams were produced in an inverted sputter source⁴ and accelerated with the Florida State University super FN tandem Van de Graaff accelerator. Beam currents of approximately 100 nA were used. The evaporated natural C target was 83 ± 10 $\mu\text{g}/\text{cm}^2$ thick. This thickness was determined by measuring the $^{12}\text{C}(^6\text{Li}, \alpha)^{14}\text{N}$ reaction at 32 MeV and comparing the observed peak yields to the reported cross sections⁵ for this reaction.

Ge(Li) detectors were used to detect the γ rays. A 100 cc detector with 2.5 keV resolution at 1.33 MeV was placed at 155° relative to the beam, and

a 40 cc detector with 3.0 keV resolution was placed at 90° . The detectors were placed 11 and 18 cm, respectively, from the target. Ge(Li) detectors were necessary in order to have sufficiently good energy resolution to resolve the 9.05–9.15–9.25 MeV triplet. Also, the good energy resolution permits Doppler-shift attenuation techniques to be used for measuring the lifetimes of the states.

Since the transfer reaction cross sections are less than 1 mb/sr for the states of interest, it was necessary to use as much Li beam as possible for the coincidence experiments. These beams result in large numbers of fast neutrons which can quickly damage the Ge(Li) detectors. To minimize the neutron flux, the beam was stopped 7 m downstream from the target. Thus, the particle detector could not be mounted at 0° as is usually done for particle- γ coincidence experiments. A second reason the particle detector could not be mounted at 0° was the similar stopping powers of Li and He particles. Normally,⁶ a stopping foil is mounted behind the target to prevent the beam from striking the detector. A foil thick enough to stop the beam in this case would have seriously degraded the energy resolution.

The simple solution would be to place the detector at 90° , but the transfer cross sections are forward peaked, so it was necessary for the particle detector to be placed at a forward angle ($\leq 20^\circ$) but not intersecting the beam. The setup which permitted these measurements is illustrated in Fig. 1. Measurements before and after the present study found the Ge(Li) detector resolutions

had degraded by ~ 0.1 keV during this study.

Standard electronics were used and have been described previously.⁶ The Ge(Li) detectors were calibrated using ^{60}Co and ^{88}Y sources placed at the target. In this way, the relative efficiencies of the detectors could be determined without having to make additional absorption corrections. The energy calibration was found stable within 2 parts in 10^4 at counting rates from 500 to 7000 Hz.

The four parameter events ($\Delta E, E, E_\gamma, \text{TAC}$) were recorded on magnetic tape for off-line sorting. A total of 2.9 million events were recorded in the $^{12}\text{C}(^6\text{Li}, ^3\text{He}\gamma)$ measurements, 3.0 million events in the $^{12}\text{C}(^7\text{Li}, \alpha\gamma)$ measurements, and 2.5 million events in the $^{11}\text{B}(^7\text{Li}, t\gamma)$ measurements.

III. DATA AND ANALYSIS

The multiparameter data were sorted to form γ -gated particle spectra and particle-gated γ -ray spectra. Figure 2 compares the γ -gated α spectrum from the $^{12}\text{C}(^7\text{Li}, \alpha\gamma)$ study to a high resolution measurement. The windows used to generate the α -gated γ -ray spectra are also shown. Accidental coincidences were subtracted to form the γ -ray spectra shown in Figs. 3–5.

Because of the small cross sections for the $^{12}\text{C}(^6\text{Li}, ^3\text{He}\gamma)$ and $^{11}\text{B}(^7\text{Li}, t\gamma)$ reactions, only the energies of the states populated could be determined from the γ -ray data. However, from the $^{12}\text{C}(^7\text{Li}, \alpha)$ reaction sufficient statistics were obtained so that centroids of the γ -ray peaks could be extracted and used to calculate the Doppler-shifted energies of the peaks. Using the reported⁷

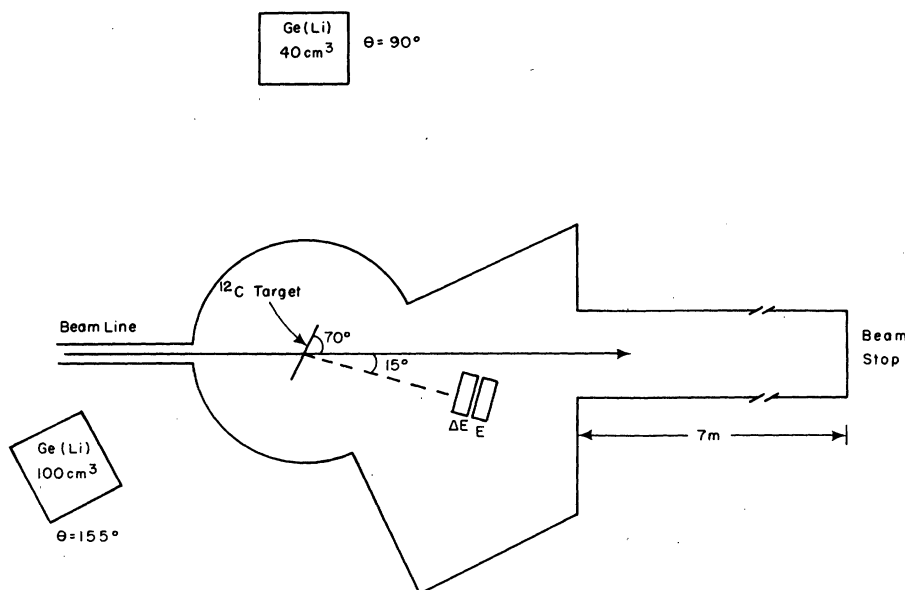


FIG. 1. Diagram of apparatus used in the present study.

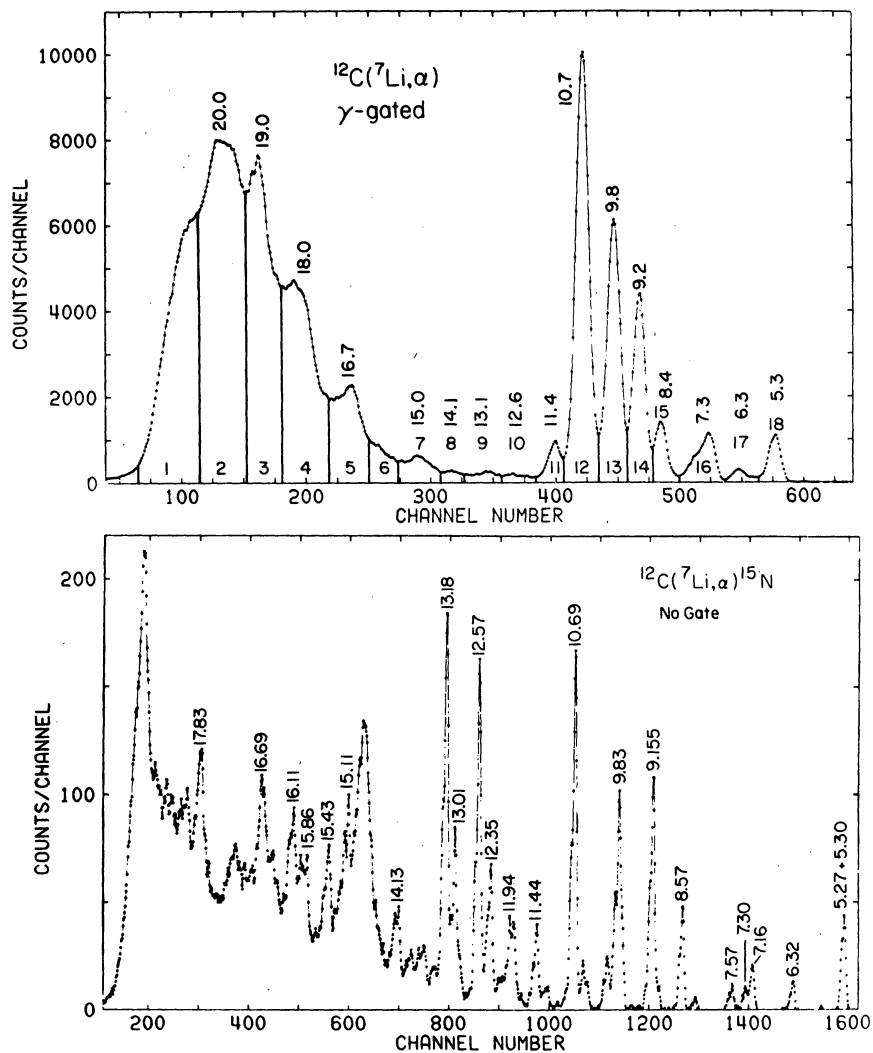


FIG. 2. Comparison of the γ -gated α -particle spectrum from the $^{12}\text{C}(^7\text{Li}, \alpha\gamma)$ reaction and a high resolution ungated α spectrum from the same reaction. Note the difference for excitation energies above 10.7 MeV. The vertical lines in the gated spectrum indicate the limits of the windows used for gating the γ rays.

energies of the transitions and the known kinematics of the reaction, it was possible to extract lifetime information from the $^{12}\text{C}(^7\text{Li}, \alpha\gamma)$ data by comparing the measured γ -ray energy shifts to the theoretical shifts calculated with the computer code FTAU.⁸ This program is based on a technique developed by Blaugrund.⁹ The resulting lifetime data are listed in Table I.

To calculate branching ratios, the γ -ray's intensities must be corrected for their anisotropies. This was done by assuming $I_{i,n}^\theta = \frac{1}{2}(I_{i,n}^{90^\circ} + I_{i,n}^{155^\circ})$ for the $^{12}\text{C}(^7\text{Li}, \alpha\gamma)$ data where $I_{i,n}^\theta$ is the intensity of transition n from state i at an angle θ relative to the beam. Because of the low coincidence rate, this could not be done for the $^{12}\text{C}(^6\text{Li}, ^3\text{He}\gamma)$ or $^{11}\text{B}(^7\text{Li}, t\gamma)$ data. Angular correlation ratios $R_{i,n} = I_{i,n}^{155^\circ}/I_{i,n}^{90^\circ}$ could be measured for seven transi-

tions in the $^{12}\text{C}(^7\text{Li}, \alpha\gamma)$ study. The other ratios could not be determined because of insufficient counting statistics. For these latter transitions, approximate ratios were used which were based on the angular correlation theory of Rose and Brink¹⁰ and the known spins of the states. The states were assumed to be aligned. The population parameters P_M necessary for these calculations were chosen to reflect the nonpolarization of the projectile and target, that is, $P_M = \frac{1}{4}$ for $|M| \leq \frac{3}{2}$ and $P_M = 0$ for $|M| > \frac{3}{2}$. These same calculations indicated that using $I_{i,n} = \frac{1}{2}(I_{i,n}^{90^\circ} + I_{i,n}^{155^\circ})$ for the stronger transitions would introduce an error of $\leq 4\%$ into $I_{i,n}$. This error was satisfactory as few of the γ rays had peak yields with smaller uncertainties. The resulting γ -ray branching ratios are compared to reported values in Table II.

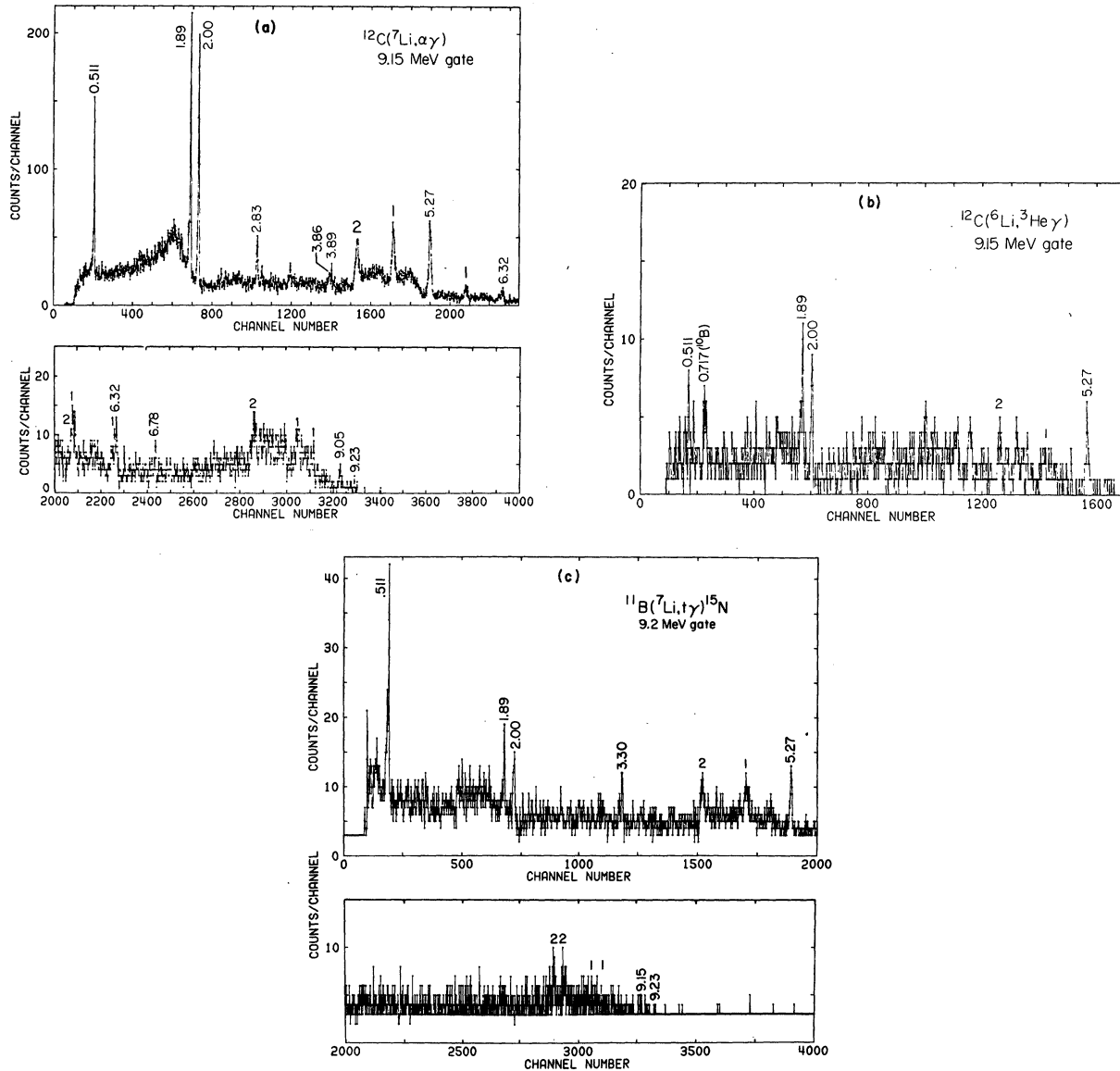


FIG. 3. Spectrum of the γ rays in coincidence with the reaction products corresponding to the 9.2 MeV excitation region in ^{15}N in the (a) $^{12}\text{C}(^7\text{Li}, \alpha\gamma)$ reaction, (b) $^{12}\text{C}(^6\text{Li}, ^3\text{He}\gamma)$ reaction, and (c) $^{11}\text{B}(^7\text{Li}, t\gamma)$ reaction. The 3.30 MeV γ ray appears in (c) because the gate region included a portion of the 8.6 MeV peak. First and second escape peaks are labeled 1 and 2, respectively.

For comparison to the nuclear model predictions, γ -ray transition strengths $\Gamma_{i,n}$ were calculated from the relation $\Gamma_{i,n} = \text{BR}_{i,n} \Gamma_i = \text{BR}_{i,n} \hbar / \tau_i$, where $\text{BR}_{i,n}$ is the branching ratio of transition n from state i and τ_i is the meanlife of the state. For the above to be true, $\sum_n \text{BR}_{i,n} = 1$.

One of the most important numbers extracted for each state was its relative reaction cross section. Since $I_{i,n} \propto \text{BR}_{i,n} \sigma_i$ where σ_i is the cross section for populating the state in the given reaction, we can obtain σ_i from $\sigma_i \propto I_{i,n} / \text{BR}_{i,n}$. The resulting relative cross sections are listed in

Table III. These results are possible because the particle- γ -ray coincidence eliminates contributions to the γ -ray intensity from feeding by higher-lying states.

IV. RESULTS

A. Relative cross sections for states populated

With the exception of the transitions from the 5.27–5.30 MeV doublet, it was possible to identify all of the final states populated in the various reactions by comparing the γ rays observed in coin-

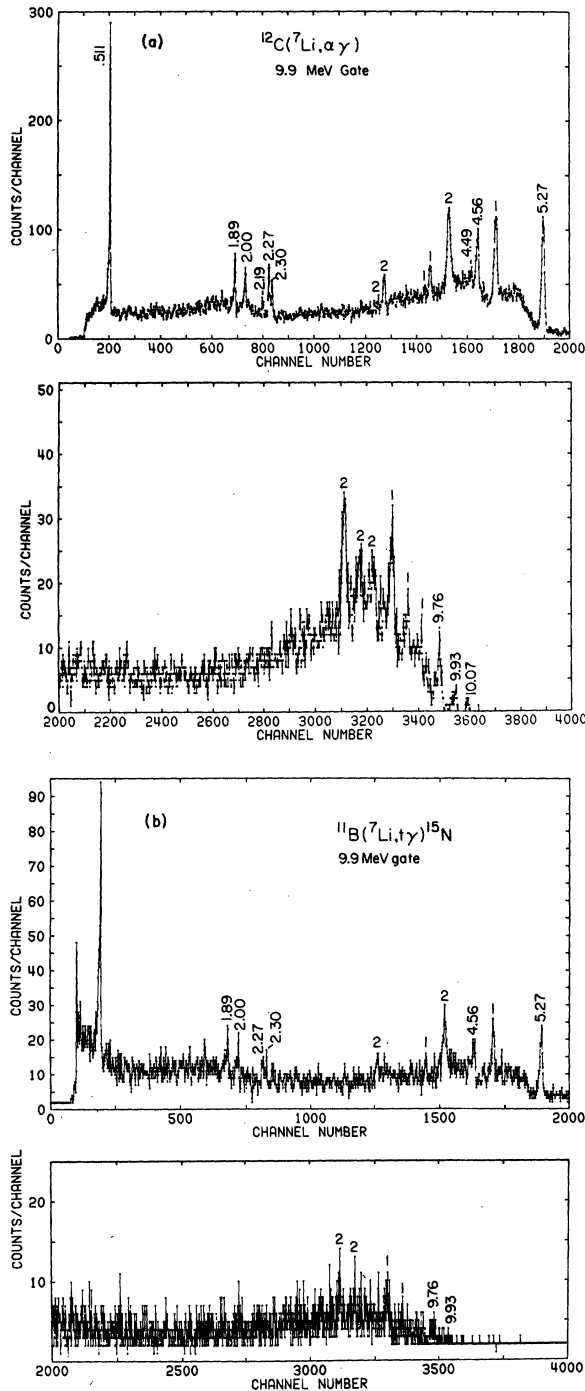


FIG. 4. Spectrum of the γ rays in coincidence with the reaction products corresponding to the 9.9 MeV excitation region in ^{15}N in the (a) $^{12}\text{C}(^7\text{Li}, \alpha\gamma)$ reaction, and (b) $^{11}\text{B}(^7\text{Li}, t\gamma)$ reaction.

cidence with a given particle group to the previously reported⁷ γ decays of the states. It is possible to determine the final state cross sections for the different reactions from high resolution particle

spectra except for the crucial 5.27–5.30 MeV, 9.152–9.155 MeV, and 10.69–10.70 MeV doublets. The reaction cross sections, branching ratios, and lifetimes for the different states will now be discussed in more detail.

1. 5.27–5.30 MeV $5/2^+ - 1/2^+$ doublet

It was not possible to resolve the ground-state transitions of these states in any of the reactions. The Doppler broadening of the γ -rays' peaks combined with the different Doppler shifts of their energies due to the very different lifetimes of the two states make the separation of the two transitions impossible. The angular correlation data from the $^{12}\text{C}(^7\text{Li}, \alpha\gamma)$ study was nonisotropic. As $\frac{1}{2}^+ \rightarrow \frac{1}{2}^+$ transitions are isotropic,¹⁰ the $\frac{5}{2}^+$ member of the doublet must have a significant cross section in this reaction. Based on comparisons to theoretical angular correlation calculations, $\sigma_{5.27}/\sigma_{5.30} \geq 2$. Without a more complete angular distribution, only this limit can be set on the ratio of the cross sections.

2. 9.152–9.155 MeV $3/2^- - 5/2^+$ doublet

As reported previously,¹¹ the $\frac{5}{2}^+$ member of the doublet is populated much stronger than the $\frac{3}{2}^-$ state in the three-particle transfer reactions. In the $^{11}\text{B}(^7\text{Li}, t\gamma)$ spectrum in Fig. 3(c), the decays of the 9.155 MeV state are seen as is the decay from the 9.152 MeV state to the ground state. We find that $\sigma_{9.155}/\sigma_{9.152} = 6 \pm 1.5$ for the $^{11}\text{B}(^7\text{Li}, t\gamma)$ reaction. The decay of the 9.23 MeV state is also observed with $\sigma_{9.23}/\sigma_{9.152} = 2.1 \pm 0.8$. The previous study¹² of this reaction at $E_{\text{Li}} = 34$ MeV did not have good enough resolution to determine this ratio.

3. 9.76–9.83–9.93 MeV triplet

The good resolution $^{12}\text{C}(^7\text{Li}, \alpha)$ data of Tserruya *et al.*¹³ show that the 9.83 MeV state is the strongest member of the 9.76, 9.83, 9.93 MeV triplet. The present data indicate that the 9.76 MeV state has significant strength as well, as it has about one half the cross section of the 9.83 MeV state in the $^{12}\text{C}(^7\text{Li}, \alpha)$ reaction. The 9.76 and 9.83 MeV states are the only known negative parity states populated strongly in the three-particle transfer reactions. The three states in the triplet are shown by the γ -ray data to be populated by the $^{11}\text{B}(^7\text{Li}, t)$ reaction as well. The 9.76 MeV state has about one tenth the $(^7\text{Li}, t)$ cross section of the 10.69 MeV state. Likewise, the 9.93 MeV state is weakly populated in the $^{11}\text{B}(^7\text{Li}, t)$ reaction.

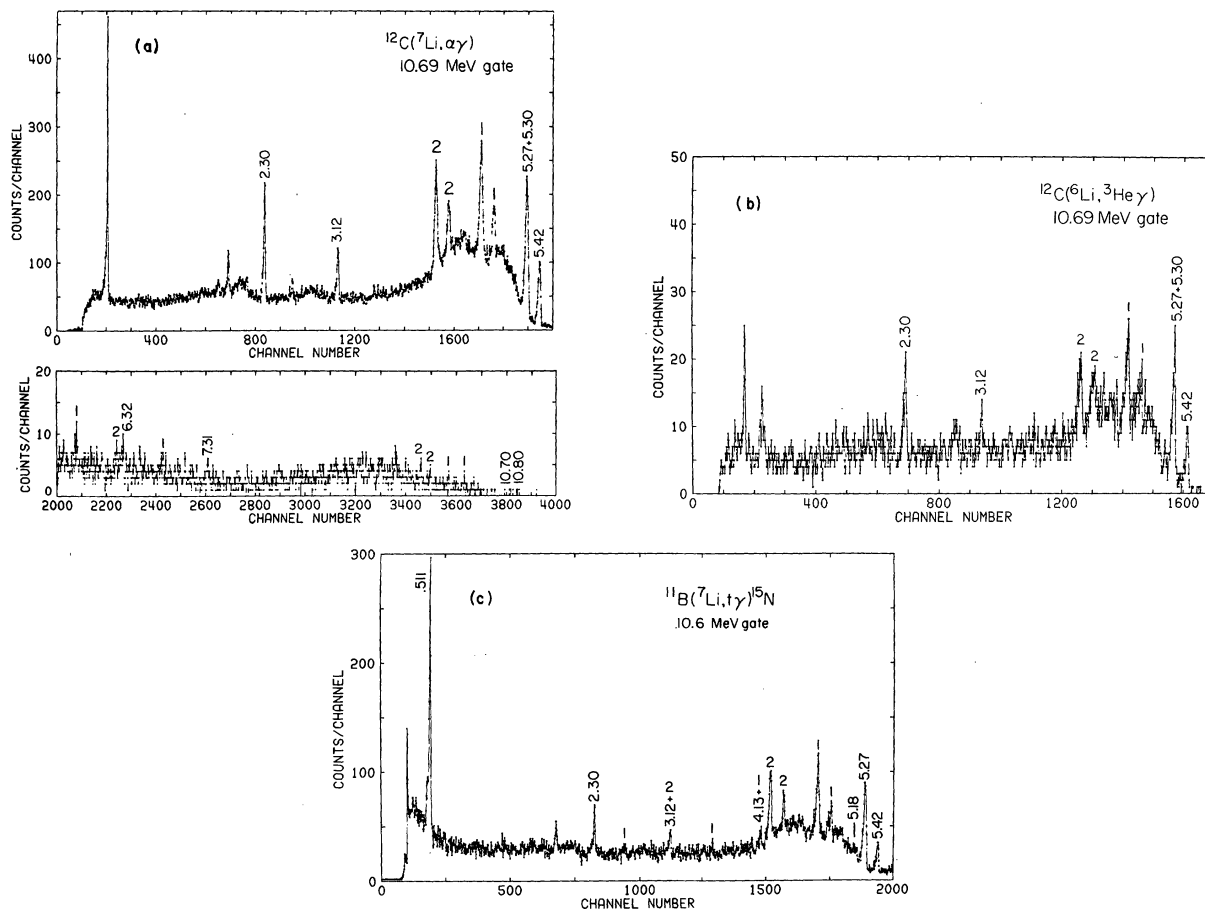


FIG. 5. Spectrum of the γ rays in coincidence with the reaction products corresponding to the 10.7 MeV excitation region in ^{15}N in the (a) $^{12}\text{C}(^7\text{Li}, \alpha\gamma)$ reaction (b) $^{12}\text{C}(^6\text{Li}, ^3\text{He}\gamma)$, and (c) $^{11}\text{B}(^7\text{Li}, t\gamma)$ reaction. The origin of the 1.89 MeV γ ray in the spectra is undetermined.

4. 10.69–10.70 MeV doublet

This doublet is the largest peak in the spectra for the $^{12}\text{C}(^6\text{Li}, ^3\text{He})$, $^{12}\text{C}(^7\text{Li}, \alpha)$, and $^{11}\text{B}(^7\text{Li}, t)$ reactions. It is therefore crucial to determine the relative cross sections of these two states before any reliable interpretation of the data can be made. Since the 10.70 MeV state has no reported decay to the 7.57 MeV state, observation of the 3.12 MeV γ ray in the spectra of Fig. 5 provides proof that the 10.69 MeV state¹⁴ is populated in the various reactions. By comparing the intensities of the 3.12 and 10.70 MeV γ rays, we find that $T = \sigma_{10.69}/\sigma_{10.70} \geq 5$ in the $^{12}\text{C}(^6\text{Li}, ^3\text{He})$ reaction, $T = 45 \pm 5$ in the $^{12}\text{C}(^7\text{Li}, \alpha)$ reaction, and $T = 7 \pm 3$ in the $^{11}\text{B}(^7\text{Li}, t)$ reaction. The 10.69 MeV state thus has large cross sections in both three- and four-particle transfer reactions.

It should be noted that a large 1.89 MeV γ ray is observed in the $^{12}\text{C}(^7\text{Li}, \alpha\gamma)$ and $^{11}\text{B}(^7\text{Li}, t\gamma)$ spectra for the 10.69 MeV excitation gate region. A weak peak was possibly identified at 1.89 MeV in the

$^{12}\text{C}(^6\text{Li}, ^3\text{He}\gamma)$ spectrum for this gate. After an extensive check of the data sorting program to eliminate the possibility that the data were misprocessed, we find that the 1.89 MeV γ ray is truly in coincidence with these portions of the particle spectra. The 7.16–5.27 MeV transition would seem a likely assignment for this γ ray, but there is no γ ray or set of γ rays in the spectra which could account for a cascade through the 7.16 MeV state. Furthermore, none of the states in this region are reported⁷ to have large decay branches through this state. The next assumption is that the γ ray results from the reactions with contaminants. This is ruled out by two facts. First, no 1.89 MeV γ rays could be found in the literature which did not have another γ ray associated with it that should have been observed in the present spectra. Second, possible contaminants lead to different final nuclei in three- and four-particle transfer reactions. At present, no satisfactory explanation to the origin of the 1.89 MeV γ ray in these spectra has been found.

TABLE I. Lifetimes of states in ^{15}N determined from $^{12}\text{C}(^7\text{Li},\alpha\gamma)$.

E_x	E_{final}	τ (fsec)	τ_{avg} (fsec)	τ_{lit} (fsec) ^a	τ_{adopted} (fsec)
10.69	5.27	17 ± 8			
	7.57	20 ± 7	18 ± 9		18 ± 9
9.93	0.0	<10	<10	<100	<10
9.83	5.27	15 ± 8			
	7.15	20 ± 8	17 ± 7	<190	17 ± 7
9.76	0.0	<12	<12		<12
9.155	5.27	17 ± 7			
	5.30	7 $^{+8}_{-6}$	7 $^{+6}_{-4}$	<10	7 $^{+6}_{-4}$
9.05	6.32	12 ± 7			
	7.16	3 $^{+7}_{-2}$			
8.57	0.0	<2	<2	<100	<2
8.31	5.27	9 ± 7	11 ± 7	<100	11 ± 7
	5.30	17 ± 7			
7.57	0.0	<16	<16	<20	<16
7.30	5.27	12 $^{+11}_{-6}$	12 $^{+11}_{-6}$	60 ± 20	60 ± 20
7.16	0.0	<10	<10	0.25 ± 0.1	0.25 ± 0.1
6.32	5.27	9 ± 7	9 ± 7	28 ± 8	18 ± 8
	0.0	<29	<29	0.22 ± 0.03	0.22 ± 0.03

^a Reference 7.TABLE II. ^{15}N γ -ray branching ratios from $^{12}\text{C}(^7\text{Li},\alpha\gamma)$.

E_x	E_{final}	BR (%) this study	BR (%) reported ^b
10.80	0.0	a	51.5 ± 0.4
10.70	0.0	a	52.6 ± 0.8
10.69	7.57	47 ± 5	36.3 ± 0.6
	5.27	53 ± 5	61.6 ± 0.3
10.07	0.0	a	96.0 ± 0.7
9.93	0.0	a	77.6 ± 1.9
9.83	7.57	11 ± 5	7.3 ± 1.0
	5.27	89 ± 5	84 ± 2
9.76	7.57	9 ± 2	5.0 ± 0.6
	5.27	24 ± 2	7.5 ± 1.5
9.23	0.0	67 ± 5	81.5 ± 2.8
	6.32	35 ± 6	24.7 ± 1.5
9.155	5.30	42 ± 8	31.2 ± 1.7
	0.0	22 ± 5	41.5 ± 2.2
9.155	7.16	57 ± 3	~50
	6.32	22 ± 2	20.0 ± 2.0
9.155	5.30	10 ± 1	~10
	5.27	11 ± 1	~8
9.05	0.0	<2	9 ± 9
	0.0	a	91.6 ± 0.9
8.57	7.16	6 ± 1	3.6 ± 0.5
	5.27	69 ± 7	65.0 ± 3.0
8.31	0.0	24 ± 4	33.0 ± 2.0
	0.0	a	79 ± 2
7.57	5.27	a	98.7 ± 1.0
7.30	0.0	a	99.3 ± 0.7
7.16	5.27	a	100.0 ± 0.4
6.32	0.0	a	100
5.27/5.30	0.0	a	100

^a Only one γ decay was observed for these states in the present data.^b Reference 7.

TABLE III. Relative cross sections of the ^{15}N states in various multiparticle transfer reactions.

E_x	J^π	$^{12}\text{C}(^7\text{Li}, \alpha)$		$^{12}\text{C}(^6\text{Li}, ^3\text{He})$		$^{11}\text{B}(^7\text{Li}, t)$	
		γ -ray data $E=28$ MeV	Particle data ^a	γ -ray data $E=34$ MeV	Particle data ^b	γ -ray data $E=28$ MeV	Particle data ^c
10.80	$\frac{3}{2}^{(*)}$	0.018 ± 0.006	0.031	
10.70	$\frac{3}{2}^-$	0.022 ± 0.007	1.000	<0.08	1.000	0.14 ± 0.04	1.00
10.69	$\frac{3}{2}^+$	1.000		1.00		1.00	
10.53	$\frac{5}{2}^+$...		0.069		...	
10.45	$\frac{5}{2}^-$	0.31 ± 0.06	0.52
10.07	$\frac{3}{2}^+$	0.017 ± 0.004	0.077	
9.93	$(\frac{1}{2}, \frac{3}{2})^+$	0.076 ± 0.010	0.072	0.03 ± 0.01	0.09
9.83	$\frac{7}{2}^-$	0.471 ± 0.020	0.668	0.75 ± 0.10	0.72	0.34 ± 0.03	0.76
9.76	$\frac{5}{2}^-$	0.220 ± 0.018		
9.23	$\frac{1}{2}^-$	0.069 ± 0.009	0.704	...	0.25	0.08 ± 0.02	0.38
9.155	$\frac{5}{2}^+$	0.469 ± 0.021		0.37 ± 0.04		0.25 ± 0.03	
9.152	$\frac{3}{2}^-$	≤ 0.010		<0.07		0.04 ± 0.01	
9.05	$\frac{1}{2}^+$	0.066 ± 0.008
8.57	$\frac{3}{2}^+$	0.125 ± 0.011	0.360	...	0.12	0.26 ± 0.03	0.12
8.31	$\frac{1}{2}^+$	0.083 ± 0.008	0.023
7.57	$\frac{7}{2}^+$	0.095 ± 0.009	0.039	0.07 ± 0.02	0.18	0.06 ± 0.01	0.05
7.31	$\frac{3}{2}^+$	0.042 ± 0.006	0.021	...	0.10	0.04 ± 0.01	0.04
7.16	$\frac{5}{2}^+$	0.265 ± 0.008	0.080	0.14 ± 0.02		0.09 ± 0.01	
6.32	$\frac{3}{2}^-$	0.069 ± 0.006	0.041	0.05
5.27/5.30	$\frac{5}{2}^+, \frac{1}{2}^+$	0.239 ± 0.009	0.365	0.35 ± 0.04	0.42	0.08 ± 0.01	0.14

^a Ratios of $d\sigma/d\Omega_{\text{max}}$ at $E_{\text{Li}} = 35$ MeV (Ref. 13).

^b Ratios of $d\sigma/d\Omega$ at $\theta_{\text{lab}} = 17.5^\circ$ and $E_{\text{Li}} = 34$ MeV (this study).

^c Ratios of $d\sigma/d\Omega$ at $\theta_{\text{lab}} = 5^\circ$ and $E_{\text{Li}} = 34$ MeV (Ref. 12).

B. Branching ratios

In the $^{12}\text{C}(^7\text{Li}, \alpha\gamma)$ study it was possible to measure the γ -ray branching ratios of many of the ^{15}N levels. The results of the present study are compared to the reported values in Table III. With the exception of the 9.23 MeV state, all of the results are in agreement with the previous values. There is some controversy over the decay of the 9.23 MeV state. Warburton *et al.*¹⁵ report that this state decays exclusively to the 5.30 MeV state. In the present work, the decays from the 9.23 MeV state to the 6.32, 5.30, and 0.0 MeV states are observed, in agreement with Phillips *et al.*¹⁶ Consequently in this work, the branching ratios of Phillips *et al.* are assumed to be correct for the 9.23 MeV state.

The states in ^{15}N above the neutron emission threshold at 10.8 MeV are shown to have small γ -decay widths ($\Gamma_\gamma/\Gamma \ll 1$) by the present data. As can be seen in Fig. 2, the singles and γ -gated

α -particle spectra are similar below 11 MeV excitation but differ markedly in the higher excitation region because the states in the 11–16 MeV excitation range decay primarily by particle emissions to the ground states of the residual nuclei.

C. Lifetimes of ^{15}N states

By measuring the Doppler shift of the γ rays it was possible to determine or to set limits on the mean lifetimes of many of the states populated in ^{15}N by the $^{12}\text{C}(^7\text{Li}, \alpha)$ reaction. Since the ^{15}N recoils were not stopped in the target, it was impossible to accurately measure lifetimes ≥ 40 fsec. The only state for which a discrepancy occurs is the 7.57 MeV state, which has an adopted value of 60 ± 20 fsec reported by Gill *et al.*,¹⁷ whereas our result is 12_{-6}^{+11} fsec. This difference in value shows the need for a more precise measurement of the lifetime of this state. For some states the γ -ray peaks were too weak to calculate the centroid

reliably, thus only upper limits could be set on the lifetimes.

The most important lifetime measured was that of the 9.155 MeV $J = \frac{5}{2}^+$ state. This state was shown to have a lifetime of 7.4^{+6} fsec in a preliminary report of this data.¹¹ This lifetime yields an $L=2$ γ -ray transition strength to the 5.30 MeV $\frac{1}{2}^+$ state which is consistent only with $E2$. Thus, the 9.155 MeV state has $J^\pi = \frac{5}{2}^+$. The lifetime information and branching ratios were combined to yield the electromagnetic transition strengths $\Gamma_{i,n}$ of the states listed in Table IV. When available, the multipole mixing ratios δ were included in the calculations; if unreported, δ was assumed to be zero.

D. The 12.84 MeV state in ^{15}O

As part of this study we have examined the relative cross sections of the various states in the different three-particle transfer reactions. Comparisons of the $^{12}\text{C}(^6\text{Li}, t)^{15}\text{O}$ and $^{12}\text{C}(^7\text{Li}, ^3\text{He})^{15}\text{N}$ cross sections by Bingham *et al.*¹⁸ for proposed mirror state pairs showed that the pairs had identical cross sections, within $\pm 5\%$ in those reactions, including the pair at 12.8–13.1 MeV in ^{15}O – ^{15}N . High resolution data at 34 MeV show that the 13.1 MeV group observed by that group in ^{15}N is in fact a doublet. Only a single peak is seen in the high resolution $^{12}\text{C}(^6\text{Li}, t)^{15}\text{O}$ spectrum of Bingham *et al.* which can correspond to the ^{15}N doublet. Martz and Parker¹⁹ observed the ^{15}N doublet and the same single peak in ^{15}O at 12.84 MeV excitation when they studied the $^{12}\text{C}(^6\text{Li}, ^3\text{He}-t)$ reactions at $E_{\text{Li}} = 40$ MeV.

On the basis of the two studies, we propose that the mirror of both members of the ^{15}N doublet are parts of the peak seen at 12.84 MeV excitation in ^{15}O . Since the data of Bingham *et al.* had an energy resolution of approximately 45 keV and the peak had the same full width at half maximum as the other peaks, we propose that the two states lie within 20 keV of each other. This is obviously an assignment based on two systematics. First, if either the 13.01 or 13.18 MeV state in ^{15}N has no mirror in ^{15}O , then it is the only state with a large three-particle transfer cross section which has no mirror. Second, if the peak in the ^{15}O spectrum is a single state and the mirror of the 13.01 MeV state in ^{15}N (the larger member of the doublet), then it is the only state in ^{15}O which has a cross section which is not virtually identical to its ^{15}N mirror at $E(^6\text{Li}) = 60$ MeV.

In summary, we propose that two states separated by 20 keV or less and strongly excited by three-particle transfer reactions exist in ^{15}O at 12.84 MeV. This same conclusion also has been reached by Martz and Parker.¹⁹

E. Summary of states observed in three-particle reactions to ^{15}N

The spectrum of states that are strongly excited in the $^{12}\text{C}(^7\text{Li}, ^3\text{He})$ and $^{12}\text{C}(^7\text{Li}, \alpha)$ reactions is shown in Fig. 6. The states populated below 10.7 MeV were determined in the present work. The spin-parity assignments were taken from the compilation of Ajzenberg-Selove,⁷ except that the positive parity assignment for the 9.155 MeV $\frac{5}{2}$ state was taken from Ref. 11. The states above 13.5 MeV were observed in a 48 MeV $^{12}\text{C}(^7\text{Li}, \alpha)$ experiment.²⁰ The limits on the spins for the states at 12.56 and 13.2 MeV come from a comparison²¹ of $^{12}\text{C}(^7\text{Li}, \alpha)$ and $^{13}\text{C}(^6\text{Li}, \alpha)$. Also, the γ -ray decay branches of these states are less than 1% of their total widths, consistent with low ($J \leq \frac{5}{2}$) spin. High spins would need large (>250 keV) single particle reduced widths to yield such small γ -decay branches, and these widths have not been observed in resonance studies of these states. A compound nucleus analysis²² of the $^{10}\text{B}(^7\text{Li}, d)^{15}\text{N}$ reaction indicates a $\frac{9}{2}^-$ assignment for these states. The negative parity assignment for these states is inconsistent with the nonpopulation of these states in the $^{13}\text{C}(^6\text{Li}, \alpha)$ reaction. The J^π assignments for the 13.0 and 15.4 MeV states come from Ref. 1 and are based on angular momentum mismatch calculations.

V. COMPARISON WITH THEORETICAL MODELS

A. Cluster model calculations

Buck *et al.*² have calculated a spectrum of ^{15}N states based on a simple $t + ^{12}\text{C}$ cluster model. These states were proposed to correspond to the states populated strongly in three-particle transfer reactions. They obtained their cluster-core interaction by folding a zero-range nucleon-nucleon interaction over the cluster and core mass distributions. They included only the $2N + L = 5$ and $2N + L = 6$ bands in their calculations where N is the number of nodes in the radial wave function and L is the orbital angular momentum quantum number.

In Fig. 6 the calculated spectrum in the model of Buck *et al.*² is compared to the states populated strongly in three-particle transfer reactions as determined in the present and previous works.^{1, 11, 13, 18, 21} The strength parameters for the potentials are those used by Buck *et al.*² in their calculations.

As reported previously,¹¹ the contention by Buck *et al.* that the 9.152 MeV $\frac{3}{2}^-$ state has a large triton transfer strength is wrong. The positive parity band is not consistent with the data either. The model predicts one $\frac{1}{2}^+$ or $\frac{3}{2}^+$ state in the 7–11 MeV

TABLE IV. γ -ray transition strengths in ^{15}N .

E_x (MeV)	J_x^π	E_{final} (MeV)	J_{final}^π	Trans. type	$\Gamma_{\text{exp.}}$ (W.u.)	Γ_{WCSM} (W.u.)
10.69	$\frac{3}{2}^+$	7.57	$\frac{7}{2}^+$	M1	$0.020_{-0.006}^{+0.013}$	0.0073
		7.16	$\frac{5}{2}^+$	E2	$0.8_{-0.3}^{+0.5}$	3.4
		5.27	$\frac{5}{2}^+$	E2	$2.6_{-0.8}^{+1.8}$	3.7
9.93	$(\frac{1}{2}, \frac{3}{2})^+$	6.32	$\frac{3}{2}^-$	E1	$>2 \times 10^{-4}$	2.8×10^{-4a}
		0.0	$\frac{1}{2}^-$	E1	$>1 \times 10^{-4}$	$\frac{1.7 \times 10^{-3a}}{3.7 \times 10^{-4b}}$
9.83	$\frac{1}{2}^-$	7.57	$\frac{7}{2}^+$	E1	$5_{-2}^{+5} \times 10^{-4}$	4.8×10^{-4}
		6.32	$\frac{3}{2}^-$	E2	$0.8_{-0.6}^{+1.2}$	1.3
		5.27	$\frac{5}{2}^+$	E1	$8_{-3}^{+6} \times 10^{-5}$	1.2×10^{-2}
9.76	$\frac{5}{2}^-$	7.57	$\frac{7}{2}^+$	E1	$>5 \times 10^{-4}$	1.2×10^{-3}
		7.16	$\frac{5}{2}^+$	E1	$>1.4 \times 10^{-4}$	1.8×10^{-4}
		6.32	$\frac{3}{2}^-$	M1	$>1.9 \times 10^{-3}$	0.27
		0.0	$\frac{1}{2}^-$	E2	>0.3	0.029
9.155	$\frac{5}{2}^+$	7.16	$\frac{5}{2}^+$	M1	$0.31_{-0.16}^{+0.27}$	0.15
		6.32	$\frac{3}{2}^-$	E1	$2.3_{-1.2}^{+1.9} \times 10^{-3}$	3×10^{-4}
		5.30	$\frac{1}{2}^+$	E2	$6.5_{-3.3}^{+6.0}$	8.8
		5.27	$\frac{5}{2}^+$	M1	$6.7_{-3.4}^{+6.0} \times 10^{-3}$	1.5×10^{-2}
9.05	$\frac{1}{2}^+$	5.27	$\frac{5}{2}^+$	E2	>1.5	...
		0.0	$\frac{1}{2}^-$	E1	$>1 \times 10^{-3}$	3×10^{-5}
		8.57	$\frac{3}{2}^+$	M1	$0.036_{-0.014}^{+0.060}$	0.035
8.57	$\frac{3}{2}^+$	6.32	$\frac{3}{2}^-$	E1	$1.7_{-1.1}^{+4.6}$	1.4×10^{-4}
		5.27	$\frac{5}{2}^+$	M1	$0.05_{-0.02}^{+0.07}$	0.42
		0.0	$\frac{1}{2}^-$	E1	$7_{-3}^{+11} \times 10^{-5}$	1.3×10^{-3}
		8.31	$\frac{1}{2}^+$	E2	>68	6×10^{-2}
7.57	$\frac{1}{2}^+$	0.0	$\frac{1}{2}^-$	E1	$>2.8 \times 10^{-3}$	9.4×10^{-3}
		5.27	$\frac{5}{2}^+$	M1	$5_{-1}^{+2} \times 10^{-2d}$	4.7×10^{-3}
				E2	$9_{-2}^{+4} \times 10^{-2d}$	1.8×10^{-2}
7.30	$\frac{3}{2}^+$	0.0	$\frac{1}{2}^-$	E3	23_{-6}^{+7d}	4.6
		5.30	$\frac{1}{2}^+$	M1	$0.03_{-0.02}^{+0.02d}$...
		5.27	$\frac{5}{2}^+$	M1	$0.1_{-0.05}^{+0.1d}$	0.19
7.16	$\frac{5}{2}^+$	0.0	$\frac{1}{2}^-$	E1	$0.016_{-0.006}^{+0.011d}$	0.0015
		5.27	$\frac{5}{2}^+$	M1	$0.26_{-0.06}^{+0.04d}$	0.33
				E2	$0.17_{-0.17}^{+0.08d}$	0.7
6.32	$\frac{3}{2}^-$	0.0	$\frac{1}{2}^-$	M1	$0.57_{-0.07}^{+0.10d}$	0.56
				E2	$2.5_{-0.3}^{+0.4d}$	0.66
5.30	$\frac{1}{2}^+$	0.0	$\frac{1}{2}^-$	E1	$4.3_{-0.9}^{+1.6} \times 10^{-4d}$	8×10^{-5}
5.27	$\frac{5}{2}^+$	0.0	$\frac{1}{2}^-$	M2	$0.69_{-0.06}^{+0.07d}$...
				E3	$7.2_{-0.6}^{+0.6d}$	0.9

^a $\frac{1}{2}^+$ of Ref. 24.

^b $\frac{3}{2}^+$ of Ref. 24.

^c $\delta = -0.028 \pm 0.012$ (Ref. 7).

^d These values were unchanged by the

results of the present study.

^e $\delta = -0.014_{-0.015}^{+0.012}$ (Ref. 7).

^f $\delta = +0.122 \pm 0.006$ (Ref. 7).

^g $\delta = -0.131 \pm 0.013$ (Ref. 7).

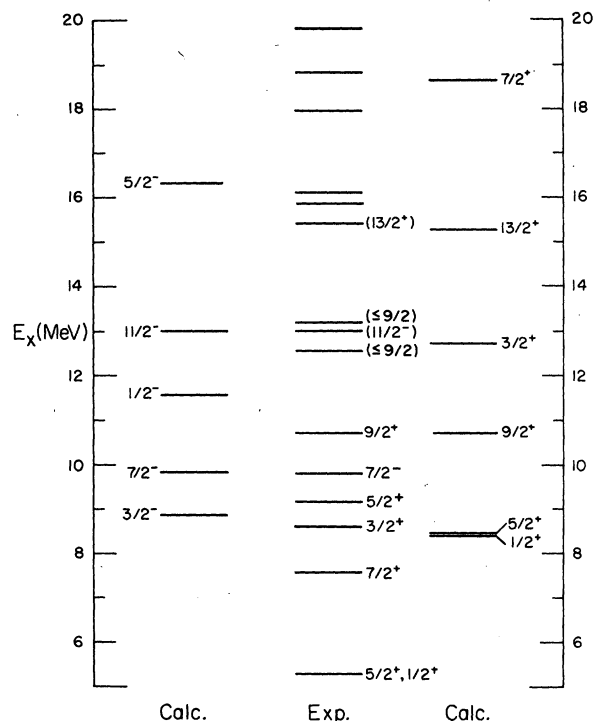


FIG. 6. Comparison of the cluster model prediction for the $2N+L=6$ (right) and $2N+L=7$ (left) triton bands in ^{15}N with the states observed experimentally to be strongly populated in three-particle transfer reactions. The parameters for the calculation are taken from Ref. 2.

excitation region. Three states with $J^\pi = \frac{1}{2}^+, \frac{3}{2}^+$ are populated with nearly equal strength in the 9–10 MeV region. If the theoretical $\frac{1}{2}^+$ state is assigned to the 9.05 MeV $\frac{1}{2}^+$ state, then there are no states to correspond to the 9.93 MeV $(\frac{1}{2}, \frac{3}{2})^+$ or 10.07 MeV $\frac{3}{2}^+$ states. The nearest theoretical $\frac{3}{2}^+$ state is nearly 3 MeV away at 12.8 MeV. Thus, we find that the simple cluster model does not reproduce the spectrum of states populated in the $^{12}\text{C}(^7\text{Li}, \alpha)$ reaction.

The simple cluster model spectrum was also calculated using the symmetrized Woods-Saxon potential of Buck and Pilt.³ This potential is given by

$$V(r) = V_0 \frac{1 + \cosh(R/a)}{\cosh(r/a) + \cosh(R/a)}.$$

The computer code BEML²³ was used to calculate the energy eigenvalues and radial wave functions. The accuracy of the code BEML was investigated by reproducing those author's calculations for ^{19}F . The energy eigenvalues were consistent within 10 keV.

Calculations for ^{15}N with R and a in the ranges $1.6 \leq R \leq 4.0$ fm and $0.8 \leq a \leq 1.5$ fm were carried

out. In each instance the value of V_0 was adjusted such that the $\frac{9}{2}^+$ state occurred at ~ 10.7 MeV. Using the values $R=2.4$ fm and $a=1.3$ fm, a spectrum is obtained which fits the lower energy positive parity spectrum much better than the folded potential of Buck *et al.*² These values are very similar to the $R=2.0$ fm and $a=1.3$ fm used by Buck and Pilt³ for ^{19}F . The $\frac{3}{2}^+$ state now occurs at 10.2 MeV which is near the 10.07 MeV $\frac{3}{2}^+$ state. Likewise, the $\frac{1}{2}^+$ state is at 8.4 MeV, fairly close to the 9.05 MeV $\frac{1}{2}^+$ state. However, there is no theoretical counterpart to the 9.93 MeV state.

More disturbing are the energies of the negative parity band. The energies of the negative parity band are poorly fitted in the model of Buck and Pilt.³ None of the parameters of the interaction potential may be varied between different $2N+L$ bands in this model. Using $R=2.4$ fm and $a=1.3$ fm and adjusting V_0 to give $E_{9/2^+} \approx 10.7$ MeV, we find that $E_{7/2^-} \approx E_{11/2^-} = 2$ MeV. This energy is 7.8 MeV below the lowest known $\frac{7}{2}^-$ state in ^{15}N and 9.7 MeV below the lowest possible $\frac{11}{2}^-$ state. These discrepancies persisted for all values of R and a investigated when the $E_{9/2^+} \approx 10.7$ MeV requirement was maintained. It was found that the symmetrized Woods-Saxon potential, like the folded potential, is unable to reproduce the spectrum of "triton cluster" states observed in ^{15}N .

As another test of the simple cluster model, the electromagnetic transition strengths of the model states were calculated. The code BEML was used to do these calculations. The equations given by Buck and Pilt³ were used which include the finite size of the cluster and core. The calculations showed that the $E2$ strengths predicted by the models are within the range $0.5 \leq \Gamma_{E2} \leq 5.0$ where Γ is given in Weisskopf units (W.u.). This range is consistent with the average $E2$ strengths for this mass region.

The $E1$ and $M1$ strengths were much larger ($0.1 \leq \Gamma_{E1} \leq 0.5$; $1 \leq \Gamma_{M1} \leq 3$) than the averages for this mass region (0.0052 for $E1$'s and 0.16 for $M1$'s). Several of the strengths are too large by two orders of magnitude when compared with the data. Buck and Pilt³ also had difficulty reproducing the experimental values for the dipole transitions in ^{19}F . We thus conclude that the simple cluster model does not reproduce the $E1$ and $M1$ strengths and that any agreement between theory and experiment for the $E2$ strength was fortuitous.

The present $^{11}\text{B}(^7\text{Li}, t\gamma)$ data serve as the final evidence that the simple cluster model is not appropriate for ^{15}N . If an analogy is made with the Buck and Pilt³ model for mass 19, the states populated by the $^{11}\text{B}(^7\text{Li}, t)$ reaction have $^{11}\text{B} + \alpha$ configurations and different states should be populated in this reaction than in the three-particle transfer

reactions. The present data show that the same states have large cross sections in both three- and four-particle transfer reactions. In particular, the 9.155, 9.83, and 10.69 MeV states are the strong members of their respective doublets in the (${}^7\text{Li}, t$), (${}^7\text{Li}, \alpha$), and (${}^6\text{Li}, {}^3\text{He}$) reactions.

B. Weak-coupling shell model

Lie, Engeland, and Dahl²⁴ have done calculations of the ${}^{15}\text{N}$ spectrum using a model that assumes the interactions between particles within a given shell are much stronger than between particles in different shells. With the confirmation¹¹ of positive parity for the 9.155 MeV $\frac{5}{2}^+$ state there is one-to-one correlation between their model states and experimentally observed states below ~10 MeV, with the exception of the 9.93 MeV ($\frac{1}{2}, \frac{3}{2}$)⁺ state for which there is neither a good spin nor parity determination. For most of the states above 10 MeV there are either no reports or conflicting reports of the spin or parity of any given state. Furthermore, the density of states (both experimental and theoretical) begins to get sufficiently high at this excitation energy that assignments become quite tenuous. Thus, the present data are compared only with the calculations for states below 11 MeV excitation.

Table IV combines the data of the present work with previous investigations to yield the γ -decay strengths of the ${}^{15}\text{N}$ states. These strengths are compared to those predicted by the weak-coupling shell model.²⁴ The calculations correctly predict the trends of the experimental values. However, many of the theoretical calculations disagree with the data by factors greater than 5. For example, the model predicts that the 8.31 MeV state will decay to the 7.16 MeV state with a strength of 0.06 W. u. while the experimental strength is >70 W. u. Most disturbing is that for the first six excited states (with 11 calculated decay strengths) only three have predicted strengths within a factor of 2 of the experimental values. On the basis of these comparisons, it appears that the weak-coupling shell model calculations of Lie *et al.*²⁴ do not serve as a good model for the electromagnetic properties of the states of ${}^{15}\text{N}$.

VI. CONCLUSIONS

The γ -ray branching ratios and lifetimes of states in ${}^{15}\text{N}$ below 10.7 MeV have been determined

in the present work. The relative cross sections for the population of states in ${}^{15}\text{N}$ by the ${}^{12}\text{C}({}^7\text{Li}, \alpha)$, ${}^{12}\text{C}({}^6\text{Li}, {}^3\text{He})$, and ${}^{11}\text{B}({}^7\text{Li}, t)$ have been determined from the observed γ -ray intensities. For the important doublets at 9.15 and 10.7 MeV, it is found that both three-particle transfer reactions populate the 9.155 ($\frac{5}{2}^+$) and 10.69 ($\frac{5}{2}^+$) states at least a factor of 5 stronger than the other members of the doublet. Also, these same two states are strongly populated in the ${}^{11}\text{B}({}^7\text{Li}, t)$ reaction. The 12.56 and 13.17 MeV states that are strongly excited in the ${}^{12}\text{C}({}^7\text{Li}, \alpha)$ reaction have γ -decay branches which are <1% of their total decay, consistent with $J \approx \frac{9}{2}$ for the states.

Comparisons between the ${}^{12}\text{C}({}^6\text{Li}, {}^3\text{He})$ spectra and cross sections and ${}^{12}\text{C}({}^6\text{Li}, t)$ suggest that there is a close-lying doublet of states at 12.8 MeV in ${}^{15}\text{O}$ that correspond to the 13.02 and 13.17 MeV states in ${}^{15}\text{N}$.

The data have been compared to a simple cluster model and to the weak-coupling shell model. The fact that the same states are populated strongly in the three- and four-particle transfer reactions shows that there is a large overlap between the proposed triton and α cluster states.^{2,3} Neither the level scheme nor γ -decay strengths were described by the simple cluster model. In fact, considering the simplicity of the model, good agreement with the data would be rather surprising. Calculations have been started²⁵ which include the effect of the strong ${}^{12}\text{C}(0, 0 \text{ MeV})$ - ${}^{12}\text{C}(4.43 \text{ MeV})$ coupling into the ${}^{15}\text{N} = {}^{12}\text{C} \otimes t$ wave functions. Weak-coupling shell model calculations give a good description of the energy spectrum of ${}^{15}\text{N}$ but do not reproduce the γ -decay strengths of the states. The applicability of the models cannot be tested for the states above 11 MeV in excitation until reliable, nonmodel-dependent determinations of the spins and parities are made.

ACKNOWLEDGMENTS

The authors would like to acknowledge many useful interactions with John Fox, Alex Lumpkin, and Gary KeKelis during the course of this work. We would also like to thank Don Robson and Doug Stanley for helpful discussions. This work was supported in part by the National Science Foundation.

- *Present address: Cyclotron Laboratory, Michigan State University, East Lansing, Michigan 48824.
- ¹N. Anyas-Weiss, J. C. Cornell, P. S. Fisher, P. N. Hudson, A. Menchaca-Roca, D. J. Millener, A. D. Pangiotou, D. K. Scott, D. Strottman, D. M. Brink, B. Buck, P. J. Ellis, and T. Engeland, *Phys. Rep.* **12C**, 202 (1974); K. Nagatani, D. H. Youngblood, R. Kene-fick, and J. Bronson, *Phys. Rev. Lett.* **31**, 250 (1973).
- ²B. Buck, C. B. Dover, and J. P. Vary, *Phys. Rev. C* **11**, 1803 (1975).
- ³B. Buck and A. A. Pilt, *Nucl. Phys.* **A280**, 133 (1977).
- ⁴K. R. Chapman, *Nucl. Instrum. Methods* **124**, 229 (1975).
- ⁵R. L. White, L. A. Charlton, and K. W. Kemper, *Phys. Rev. C* **12**, 1918 (1975).
- ⁶J. KeKelis, A. H. Lumpkin, K. W. Kemper, and J. D. Fox, *Phys. Rev. C* **15**, 664 (1977).
- ⁷F. Ajzenberg-Selove, *Nucl. Phys.* **A268**, 1 (1976).
- ⁸R. W. Zurmühle, D. A. Hutcheon, and J. J. Weaver, *Nucl. Phys.* **A180**, 417 (1972); R. W. Zurmühle, private communication.
- ⁹A. E. Blaugrund, *Nucl. Phys.* **88**, 501 (1966).
- ¹⁰H. J. Rose and D. M. Brink, *Rev. Mod. Phys.* **39**, 306 (1967).
- ¹¹L. H. Harwood, K. W. Kemper, J. D. Fox, and A. H. Lumpkin, *Phys. Rev. C* **18**, 2145 (1978).
- ¹²G. A. Norton, K. W. Kemper, G. E. Moore, R. J. Puigh, and M. E. Williams-Norton, *Phys. Rev. C* **13**, 1211 (1976).
- ¹³I. Tserruya, B. Rosner, and K. Bethge, *Nucl. Phys.* **A213**, 22 (1973).
- ¹⁴R. P. Beukens, T. E. Drake, and A. E. Litherland, *Phys. Lett.* **56B**, 253 (1975).
- ¹⁵E. K. Warburton, J. W. Olness, and D. E. Alburger, *Phys. Rev.* **140**, B1202 (1965).
- ¹⁶G. W. Phillips, F. C. Young, and J. B. Marion, *Phys. Rev.* **159**, 891 (1967).
- ¹⁷R. D. Gill, J. G. Lopes, O. Hauser, and H. J. Rose, *Nucl. Phys.* **A121**, 209 (1968).
- ¹⁸H. G. Bingham, M. L. Halbert, D. C. Hensley, E. Newman, K. W. Kemper, and L. A. Charlton, *Phys. Rev. C* **11**, 1913 (1975).
- ¹⁹L. M. Martz and P. D. Parker, private communication.
- ²⁰A. F. Zeller, K. W. Kemper, T. R. Ophel, and A. Johnston, in *Proceedings of the International Conference on Nuclear Structure, Tokyo, 1977*, edited by T. Marumori (Phys. Soc. of Japan, Tokyo, 1978), p. 175.
- ²¹L. H. Harwood and K. W. Kemper, *Phys. Rev. C* **14**, 368 (1976).
- ²²W. Kohler, H. Schmidt-Böcking, and K. Bethge, *Nucl. Phys.* **A262**, 113 (1976).
- ²³L. H. Harwood, FORTRAN IV Computer Code BEML (unpublished).
- ²⁴S. Lie, T. Engeland, and G. Dahll, *Nucl. Phys.* **A156**, 449 (1970); S. Lie and T. Engeland, *ibid.* **A169**, 617 (1971); **A267**, 123 (1976).
- ²⁵D. Stanley, private communication.